Solid State Phenomena
ISSN: 1662-9779, Vol. 303, pp 161-168
doi:10.4028/www.scientific.net/SSP.303.161

Submitted: 2019-12-18
Accepted: 2019-12-18
Online: 2020-05-04

Structural-Phase State of UFG-Titanium Implanted with Aluminum Ions

A.V. Nikonenko[1,a], N.A. Popova[2], E.L. Nikonenko [2,3], M.P. Kalashnikov [3,4], and I.A. Kurzina[5]

[1]Tomsk State University of Control Systems and Radioelectronics, 40 Lenina Avenue, Tomsk, 634050, Russia

[2]Tomsk State University of Architecture and Building, 2 Solyanaya Square, Tomsk, 634003, Russia

[3]National Research Tomsk Polytechnic University, 30 Lenina Avenue, Tomsk, 634050, Russia

[4] nstitute of Strength Physics and Materials Science (ISPMS) SB RAS, 2/4, pr. Akademicheskii, Tomsk, 634055, Russia

[5]National Research Tomsk State University, 36 Lenina Avenue Tomsk, 634055, Russia

E-mail: [a]aliska-nik@mail.ru

Keywords: titanium, scanning electron microscopy, structure.

Abstract. Transmission electron microscopy investigations were carried out to study the structural-phase state of ultra-fine grain (UFG) titanium with the average grain size of ~0.2 μm, implanted with aluminum ions. Implantation was carried out on MEVVA-V.RU ion source at room temperature, exposure time of 5.25 h and ion implantation dosage of $1 \cdot 10^{18}$ ion/cm^2. UFG-titanium was obtained by a combined multiple uniaxial compaction with rolling in grooved rolls and further annealing at 573 K for 1h. The specimens were investigated before and after implantation at a distance of 70-100 nm from the specimen surface. Concentration profile of aluminum implanted with α-Ti was obtained. It was revealed that the thickness of implanted layer was 200 nm, while maximum aluminum concentration was 70 at.%. Implantation of aluminum into titanium has resulted in formation of the whole number of phases having various crystal lattices, like β-Ti, $TiAl_3$, Ti_3Al, TiC and TiO_2. The areas of their localization, the sizes, distribution density and volume fractions were determined. Grain distribution functions by their sizes were built, and the average grain size was defined. The paper investigates the influence of implantation on the grain anisotropy factor. It was revealed that implantation leads to the decrease in the average transverse and longitudinal grain size of α-Ti and decrease in the anisotropy factor by three times. The yield stress and contributions of separate strengthening mechanisms before and after implantation were calculated. The implantation has resulted in increase in the yield stress by two times.

1. Introduction

Titanium has been known to possess good mechanical properties, such as high mechanical strength, high corrosion resistance, and relatively low density. Due to that, titanium and its alloys are currently occupying the leading position among structural materials in various fields of modern industry. Surface modification is used to enhance mechanical, physical and operational properties of titanium. The methods of materials processing with metal ion beams are one of the most intensively developing directions of new materials synthesis [1–4].

It is known that introduction of aluminum into titanium alloys is accompanied by the formation of nanoparticles of intermetallic phases, such as Ti_3Al and TiAl [3]. Intermetallic phases of Ti-Al system have high mechanical strength, hardness; wear and corrosion resistance [5–6]. Formation of nano-particles of intermetallic phases in the structure of titanium-based alloy under conditions of ion implantation leads to significant strengthening of this material conditioned by both disperse strengthening and by occurrence of internal stress fields [7]. Therefore, based on intermetallic compounds, such as Ti_3Al and TiAl, it is possible to create corrosion- and heat-resistant materials of a new type which can operate within the temperature interval of 600-900°C and are able to replace even super-alloys. It is also known that introduction of aluminum into titanium alloys improves not

only their mechanical properties under various temperatures but it also significantly increases their oxidation resistance [8].

The present work aims to conduct quantitative comparative analysis of microstructure and phase composition of titanium target in ultrafine grain (UFG) state before and after implantation with aluminum ions and to calculate the strength components of ion-doped UFG-titanium layers comprising the yield stress.

2. Materials and Methods

Commercially pure titanium VT1-0 (Russian grade) with the average grain size of ~0.2 μm was used as the material under study. The alloy has hexagonal close-packed (hcp) crystal lattice (α-Ti). Ultra-fine grain state in titanium specimens was formed using combined method of multiple uniaxial compaction [9]. The number of press moldings was equal to three. The temperature of compaction in each cycle was constant, but at transition from the previous compaction to the next one it decreased gradually within the interval of 500 – 400 K. Deformation velocity at compaction was 10^{-2}–10^{-1} s^{-1}. Deformation value at single compaction was equal to 40–50 %. With each next compaction the specimen was rotated by 90°. The value of cumulative deformation e = 2.12. After the compaction stage titanium specimens were subjected to deformation by multipass rolling in grooved rolls at room temperature. The value of cumulative deformation at rolling was 75 %. In order to increase titanium plasticity annealing was held at the temperature of 573 K during 1 h. The structural state of titanium was almost not changed following annealing, however its tensile ductility increased by 6–8 % [10–11].

Ion implantation of titanium with aluminum ions was conducted using MEVVA-V.RU ion source at temperature of 623 K, accelerating voltage of 50 kV, current density of ion beam of 6.5 mA / cm^2, the distance of 60 cm from ion-optical system, implantation time 5.25 h and ion implantation dosage of $1 \cdot 10^{18}$ ion / cm^2. The analysis of chemical composition of implanted materials was held using Augen electron spectrometer 09IOS. Microstructure and phase composition were investigated using transmission electron microscopy (TEM) by means of electron microscope EM-125 at accelerating voltage of 125 kV. Working increase in microscope column was equal to 25000 – 76000 times. The specimens were investigated in two states: 1) before implantation (original state) and 2) after implantation at the distance of 70–100 nm from the specimen surface.

Phase analysis was conducted upon the images proved by micro-diffraction patterns and dark-field images obtained in respective reflexes. All the parameters were determined using standard methods. The obtained data was processed statistically.

3. Results and Discussion

TEM investigations revealed that in the original state the structure of material has grains of anisotropic shape with clearly distinguished texture (Fig.1*a*). Anisotropic shape of grains is attributed to the method of UFG-titanium formation. Bar charts of distribution of transverse (d) and longitudinal (L) grain sizes are given in Fig. 1*b*-*c*.

Transverse grain size (Fig.1*b*) is within the interval of 0.05–0.30 μm. About 75 % of the bulk is occupied by the grains sized less than 0.2 μm. The average grain size is 0.15±0.02 μm. Longitudinal grain size (Fig.1*c*) lies within the interval of 0.1–6.0 μm. The average longitudinal size has the value of 1.9 ± 0.6 μm. Anisotropy factor k = L/d is 12.9. Cumulative distribution curve for transverse and for longitudinal grain sizes is unimodal; its maximum is close to the average value.

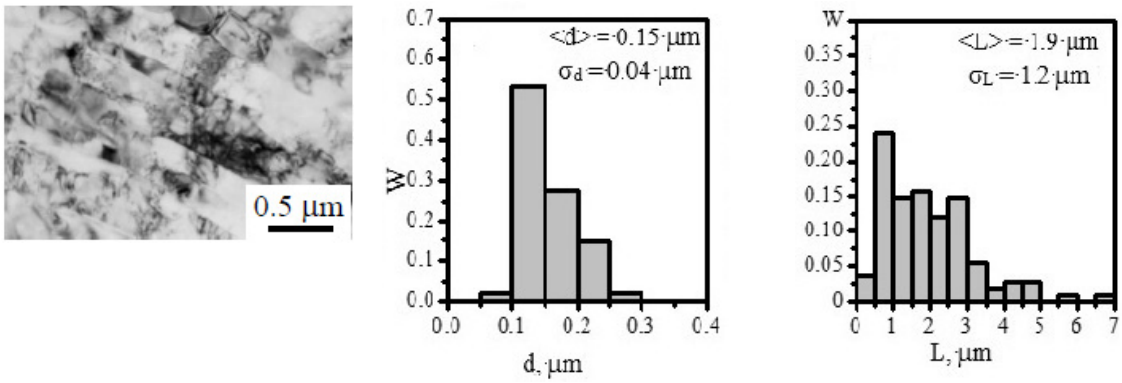

a b c

Figure 1. Electron-microscopic image (*a*) and distributions upon sizes of transverse d (*b*) and longitudinal L (*c*) grains in VT1-0 alloy before implantation

TEM investigations have established that in the initial stage VT1-0 alloy is presented by the grains of α-Ti phase (spatial group P63/mmc). Along with the grains of α-Ti in the alloy structure other grains were found in the smaller amount (0.9% of the material bulk), those grains have bcc crystal lattice (spatial group Im3m) and have the shape of lamellar precipitates. Formation of β-Ti phase occurs during the alloy manufacturing, i.e. in the conditions of intensive plastic deformation and further annealing at 573 K at transformation of α-Ti → β-Ti. β-Ti precipitations locate along the longitudinal grain boundaries α-Ti (Fig.2). Their average grain size is 50 × 200 nm, volume ratio is ~1 %.

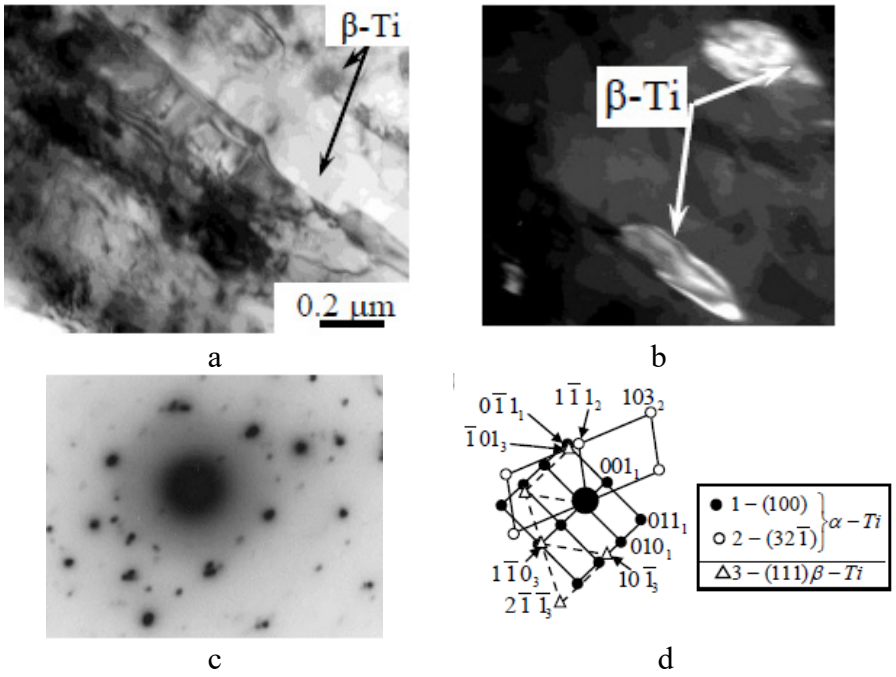

a b c d

Figure 2. Electron-microscopic image of the original structure of UFG-titanium: *a* – bright-field image; *b* – dark-field image, obtained in the $[1\bar{1}0]$ reflex of β-Ti phase; *c* – micro-diffraction pattern obtained from the area (*a*); d – its indicated scheme

The value of average scalar dislocation density in α-Ti grains equals to $7.5 \cdot 10^{-14}$ m^{-2}. Such high scalar dislocation density is attributed to the fact that in longitudinal section titanium specimen after compaction and multipass rolling fine structure of α-Ti has the form of band-type substructure. As known in [12], band-type substructure is always characterized by high value of scalar dislocation density. The average value of shear internal stresses in the original state of α-Ti is 390 MPa.

Excess dislocation density and internal moment (local) stresses, induced by excess dislocation density, were not found. It is proved that inside the α-Ti grains bend extinction contours were not revealed.

4. Phase composition and the structure of UFG-titanium after ion implantation

Implantation with aluminum ions has led to modification of the surface layer of VT1-0 alloy. Concentration profile of aluminum obtained by Augen spectrometer is illustrated in Fig. 3, in the course of removing from the surface of alloy.

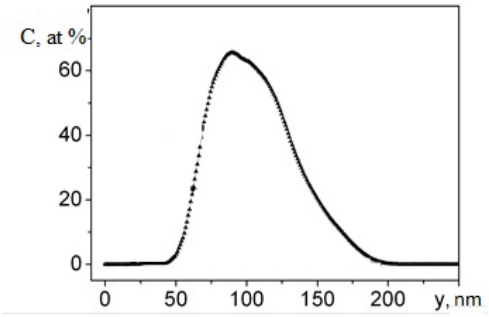

Figure 3. Concentration profile of aluminum obtained in the course of removing from the implanted surface of the alloy

As can be seen from Fig. 3, the maximum aluminum concentration at implantation dosage of $1 \cdot 10^{18}$ ion / cm^2 is about 70 at. %; the thickness of implanted layer is 200 nm. Implantation resulted in the change in grain composition of the alloy (Fig. 4*a*). Particularly, the average longitudinal grain size α-Ti decreased and now has the value of <L> = 0.7 ± 0.1 μm. In this case, grain distribution upon the L sizes remains unimodal. The maximum of distribution function is still close to the average value (Fig.4*b*). The average transverse grain size remained almost unchanged (<d> = 0.12 ± 0.02 μm). Grain distribution along the d sizes also remains unimodal, and the maximum of distribution function also lies close to the average value (Fig. 4*c*). Anisotropy factor decreased by over two times and now has the value of k = 5.7, i.e. the grains α-Ti become more equiaxial. Thus, aluminum implantation into titanium primarily leads to the formation of transverse boundaries in the grains; afterwards, longitudinal grains are formed.

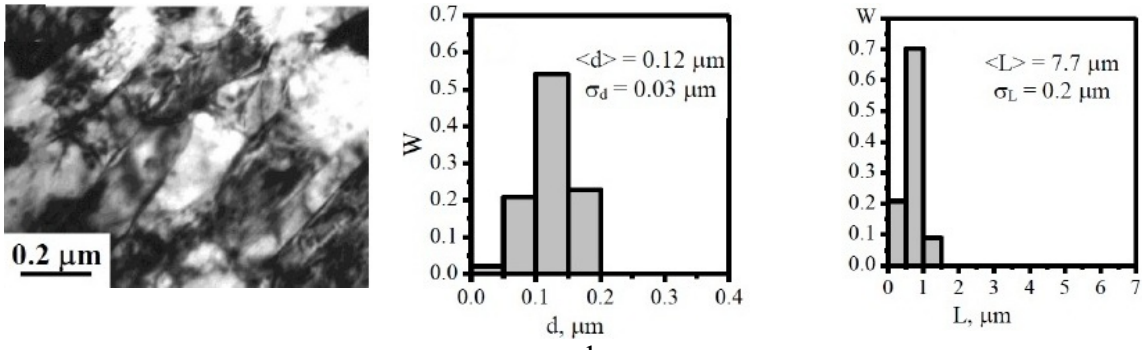

a b c

Figure 4. Electron-microscopic image (*a*) and grain distribution along sizes in VT1 - 0 alloy after implantation: transverse d (*b*) and longitudinal L (*c*)

TEM investigations revealed that the implanted layer is given, like in the original state, by α-Ti phase grains with hcp crystal lattice and spatial group P63/mmc. Along with the α-Ti grains in the structure of alloy there are β-Ti grains. β-Ti grains also have the form of lamellar precipitates, located along the longitudinal boundaries of α-Ti grains. The width of separate plates is 50 nm on average, the
length is 200 nm, and volume ratio is 0.9%. Therefore, concentration areas, the shape, sizes and volume ratio of β-Ti grains are the same as in the original state of the alloy (Fig. 2).

Conducted studies demonstrated that aluminum ion implantation into titanium resulted in formation of the number of phases: Ti_3Al, $TiAl_3$, TiO_2, TiC.

Ti_3Al phase is an ordered phase with $D0_{19}$ superstructure and it has hcp crystal lattice. Particles of Ti_3Al phase have lamellar shape and are located along the longitudinal boundaries of α-Ti grains (Fig.5). The average particle size is 15 × 70 nm, volume ratio is 1.5%.

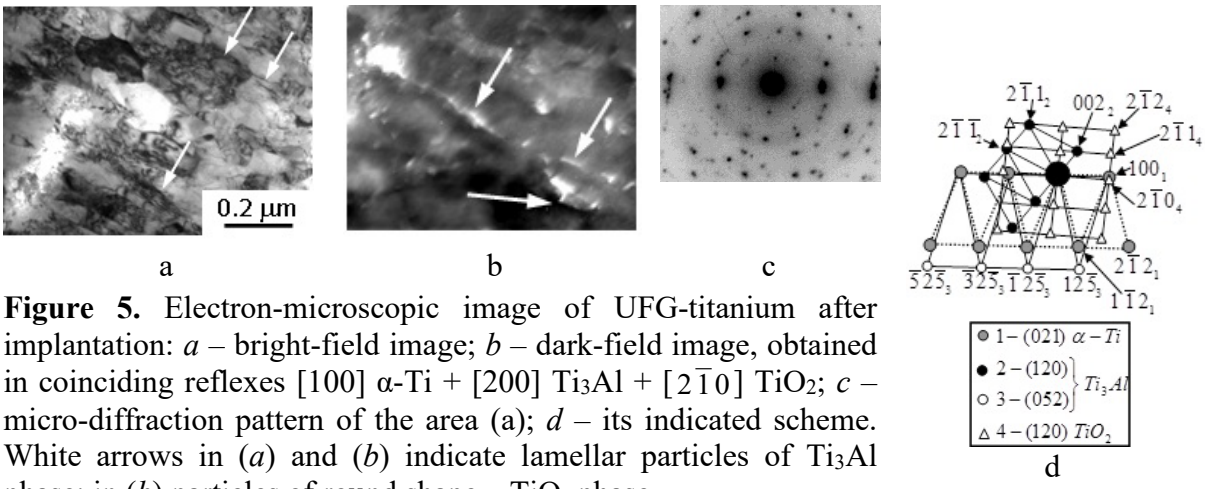

Figure 5. Electron-microscopic image of UFG-titanium after implantation: *a* – bright-field image; *b* – dark-field image, obtained in coinciding reflexes [100] α-Ti + [200] Ti_3Al + $[2\bar{1}0]$ TiO_2; *c* – micro-diffraction pattern of the area (a); *d* – its indicated scheme. White arrows in (*a*) and (*b*) indicate lamellar particles of Ti_3Al phase; in (*b*) particles of round shape – TiO_2 phase

$TiAl_3$ phase is also an ordered phase with $D0_{22}$ superstructure, having body-centered tetragonal crystal lattice with spatial group I4/mmm. It is predominantly formed in the shape of rounded particles, their average size being 120 nm. The particles of this phase are located in the joints and along the boundaries of α-Ti grains (Fig. 6). The volume ratio of this phase does not exceed 2% of the material bulk.

Along with the aluminide phases in the implanted layer there are also oxide and carbide precipitations. Titanium oxide TiO_2 (or brookite), has orthorhombic crystal lattice (spatial group Pbca). TiO_2 particles have rounded shape and are separated on dislocations (Fig.7) and along the boundaries of α-Ti grains (Fig.5). TiO_2 particles on dislocations have the size of 15 nm. Their volume ratio is 0.8 %. Along the grain boundaries particles have the size of 10 nm, and their volume ratio is 0.3%.

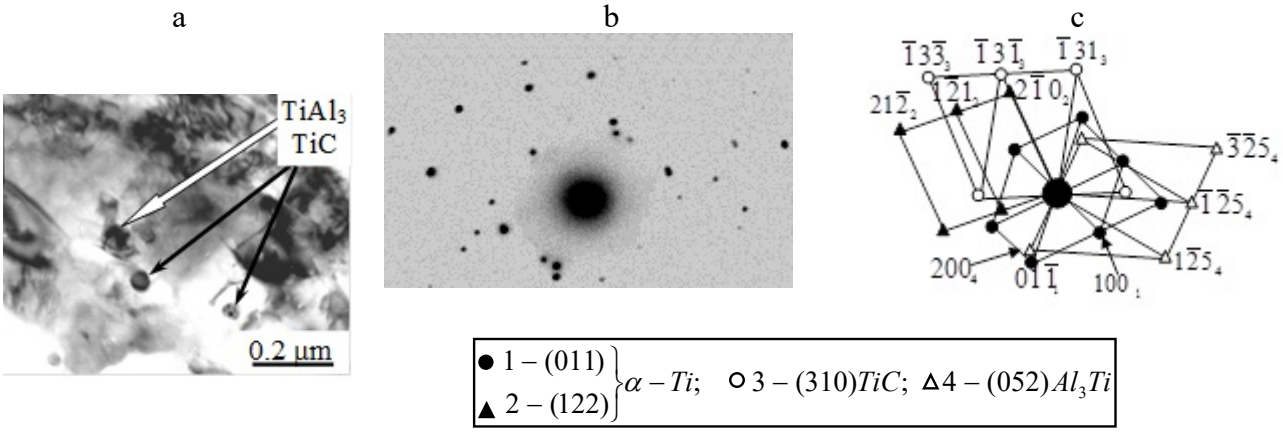

Figure 6. Electron-microscopic image of UFG-titanium after implantation: *a* – bright-field image; *b* – micro-diffraction pattern of the area (*a*); *b* – its indicated scheme. Black arrows in (*a*) indicate rounded particles of TiC phase, white arrows show rounded particles of $TiAl_3$ phase

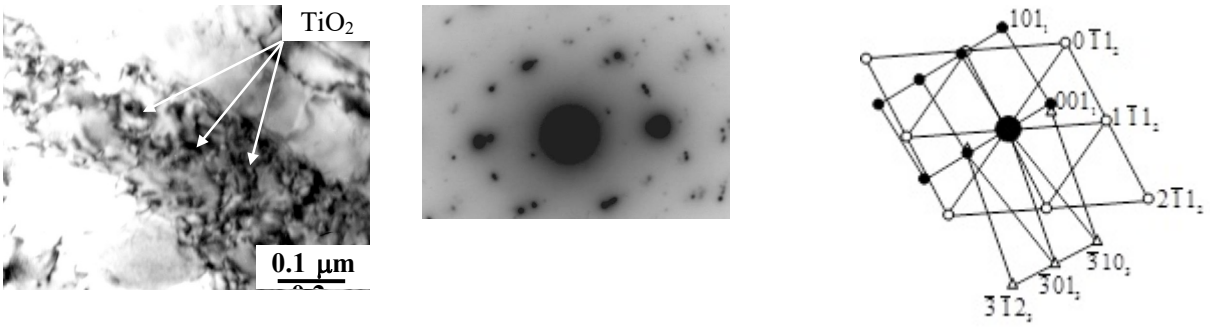

a b c

Figure 7. Electron-microscopic image of UFG-titanium after implantation: *a* – bright-field image; *b* – micro-diffraction pattern of the area (*a*); *c* – its indicated scheme. White arrows in (*a*) indicate particles of TiO_2 phase

Titanium carbide TiC has fcc crystal lattice (spatial group Fm3m). The particles of titanium carbide TiC have rounded shape and are located inside the α-Ti grains (Fig. 6). The average particle size of TiC phase equals to 15 nm, their volume ratio is 0.5%.

In the implanted layer in α-Ti grains there are dislocations. Dislocation substructure is mainly lattice-like. The average scalar dislocation density is higher than in the original state and it has the value of $8.5 \cdot 10^{14}$ m^{-2}. The formed dislocation density creates internal stresses (shear stresses). The amplitude of internal stresses was equal to 410 MPa, which is higher than in the original state. Long-range stress fields are still not found.

5. Calculation of Yield Stress

According to the obtained quantitative data for the original and implanted states calculation of strength components comprising the yield stress was carried out. It was calculated by the formula where contributions of strengthening from internal stresses (shear and moment stresses) are added quadratically, the other contributions are summed additively [13]:

$$\sigma = \Delta\sigma_{fr} + \Delta\sigma_{sol} + \Delta\sigma_{g} + \Delta\sigma_{Or} + \sqrt{\Delta\sigma_{F}^{2} + \Delta\sigma_{I}^{2}}\,, \qquad (1)$$

where $\Delta\sigma_{fr}$ is friction stress of dislocations in crystal lattice of α-Ti; $\Delta\sigma_{sol}$ is strengthening of UFG-Ti solid solution with atoms of alloying elements (Al, C, O); $\Delta\sigma_{F}$ is strengthening of "forest" dislocations which are intersecting gliding dislocations (internal shear stresses); $\Delta\sigma_{I}$ is strengthening with long-range stress fields, formed by excess dislocation density (internal moment stresses); $\Delta\sigma_{Or}$ is material strengthening with non-coherent particles when they are by-passed by dislocations according to Orowan mechanism; $\Delta\sigma_{g}$ is strengthening due to grain boundaries.

Calculation of the yield stress was carried out before and after implantation. In the original state the alloy under study with the average grain size of ~0.2 μm is completely single-phased, therefore the contribution into strengthening attributed to the presence of secondary phases $\Delta\sigma_{Or}$ was not found. Also, in the original state bend extinction contours were not observed, which testify on the presence of internal moment stresses and therefore strengthening with long-range stress fields $\Delta\sigma_{I}$ is completely absent. The components $\Delta\sigma_{fr}$ and $\Delta\sigma_{sol}$ contribute to the general strengthening to the minimum extend, as according to Augen spectroscopy and X-ray crystallographic analysis [14], in the solid solution carbon and oxygen were not found. Therefore, strengthening of material before implantation will be determined only by $\Delta\sigma_{g}$ (grain boundary strengthening) and $\Delta\sigma_{F}$ ("forest" dislocations strengthening). Grain boundary strengthening $\Delta\sigma_{g}$ is described by Hall-Petch-type relationship [15]: $\Delta\sigma_{g} = k \times d^{-0.5}$, where k is coefficient (0.3 МПа·м$^{1/2}$), d is the grain size α-Ti.

It was mentioned above that implantation of α-Ti has lead to the decrease in the grain size. Thus, contribution of the grain boundary strengthening after implantation slightly increases (Table

1). Great contribution into strengthening of implanted α-Ti is given by "forest" dislocations. It is known that non-charged dislocation ensemble is an ensemble without excess dislocations, when $\rho_+ = \rho_-$ and then excess dislocation density $\rho_\pm = \rho_+ - \rho_- = 0$. In this case non-charged dislocation ensemble induces shear stress (stress fields, created by dislocation structure), which is determined by the formula [13]:

$$\Delta\sigma_l = m\alpha Gb\sqrt{\rho}\,, \tag{2}$$

where *m* is orientation multiplying factor, α is proportionality factor, characterizing the intensity of interdislocation interactions (depends on the type of dislocation substructure), G – shear modulus, b – Burgers vector, ρ – dislocation density.

In case of charged dislocation ensemble, when $\rho_\pm = \rho_+ - \rho_- \neq 0$, excess dislocation density results in occurrence of long-range stresses which are indicated by the presence of bend extinction contours in material. It has been revealed that after α-Ti implantation like in the original state, bend extinction contours are not found in the material, therefore $\Delta\sigma_l = 0$.

Implantation has lead to the formation of a number of secondary phases. Specifically, the particles Ti_3Al $TiAl_3$, TiC, TiO_2 are formed, along with β-Ti, located along the boundaries and inside the grains. Contribution of dispersion strengthening is calculated as in [16]: $\Delta\sigma_{Or} = Gb/r$, where G – shear modulus, b – Burgers vector, r – distance between particles.

As a result, material strengthening after implantation will be defined as follows: $\Delta\sigma_g$, $\Delta\sigma_F$ and $\Delta\sigma_{Or}$.

Table 1. Yield stress and dispersion strengthening before and after implantation of VT1-0 alloys

Δσ, MPa				
σ	$\Delta\sigma_g$	$\Delta\sigma_F$	$\Delta\sigma_l$	$\Delta\sigma_{Or}$
Original state				
925	537	388	0	0
Implanted α-Ti				
1517	537	414	0	566

As can be seen from the table the yield stress after implantation increased. In UFG-titanium in the original state the yield stress was 925 MPa, and after implantation it increased by almost twice.

6. Conclusion

Conducted TEM investigations established that implantation of titanium with aluminum ions results in reduction of grain anisotropy and in the formation of poly-phase implanted layer based on UFG-titanium grains containing aluminide ordered phases (Ti_3Al and $TiAl_3$), as well as oxide phases (TiO_2) and carbide phases (TiC). Ti_3Al phase is formed in the shape of lamellar precipitates along the grain boundaries α-Ti. $TiAl_3$ phase is localized in the shape of rounded particles in triple joints and along the grain boundaries of α-Ti. The particles of TiO_2 have rounded shape and are located on the dislocations inside the α-Ti grains, as well as on their boundaries. TiC particles are located inside the α-Ti grains. A significant change in the structure is connected, primarily, with the energy impact in the conditions of implantation, specifically with the local temperature rise in implantation conditions.

It has also been found that implantation results in increase in the scalar dislocation density and internal stresses, induced by dislocation structure, however they do not lead to polarization of dislocation structure.

The research has been carried out with the financial support of Russian Foundation for Basic Research, Project № 19-08-01041.

References

[1] Hirvonen J K 1985 *Ion implantation* (Moscow:Metallurgiya Publ) p 245

[2] Brown G 1989 *Nucl Instr Meth* B37/38 68–73

[3] Nikonenko A V, Popova N A, Nikonenko E L and Kurzina I A 2019 *Conf Proc Physics* 1 253-5

[4] Komarov F F 2001 *Physical processes at ion implantation in solid bodies* (Minsk: Tekhnoprint Publ) p 392

[5] Kurzina I A, Popova N A, Nikonenko E L, Kalashnikov M P, Savkin K P, Sharkeev Y P and Kozlov E V 2012 *Izvestiya RAN. Physics*. 76 № 1 74–8

[6] Andrievskii R A and Ragulya A V 2005 *Nanostructural materials: Studybook for university students* (Moscow, Akademiya Publ) p 192

[7] Kurzina I A, Sharkeev Y P and Kozlov E V 2007 *Structure and properties of perspective materials* ed A I Potekaev (Tomsk: NTL Publ) p 195

[8] Tsiganov I, Wieser E, Matz W, Mücklich A, Reuther H, Pham M T and Richter E 2000 *Thin Solid Films* 376 188–97

[9] Eroshenko A Y, Sharkeev Y P, Tolmachev A I, Korobitsyn G P and Danilov V I 2009 *Perspective materials* S7 107–12

[10] Sharkeev Y P, Eroshenko A Y, Bratchikov A D, Legostaeva E V and Kukareko V A 2005 *Physical mesomechanics* 8 № S 91–4

[11] Fedorischeva M V, Kalashnikov M P, Nikonenko A V and Bozhko I A 2018 *Vacuum* 149 150-5.

[12] Koneva N A and Kozlov E V 1990 *Izvestiya vuzov. Fizika* 33 № 2 89–106

[13] Koneva N A and Kozlov E V 1991 *Izvestiya vuzov. Fizika* 3 56-70

[14] Kurzina I A, Bozhko I A, Popova N A et al 2012 *Conf. Proc* (Rostov-on-Don SKNT VS UFU APSN Publ) 180-83

[15] Mak Lin D 1965 *Mechanical properties of metals* (Moscow: Metallurgiya) p 431

[16] Popov L E, Kovalevskaya T A, Koneva N A and Popov V L 1979 *FMM Publ* 47 № 2 396-03